Original Article

JCBFM

Journal of Cerebral Blood Flow & Metabolism
2021, Vol. 41(3) 569–578

DOI: 10.1177/0271678X20915403
journals.sagepub.com/home/jcbfm


Repeatability of parametric methods for [^{18}F]florbetapir imaging in Alzheimer's disease and healthy controls: A test–retest study

Sander CJ Verfaillie[1,*], Sandeep SV Golla[1,*], Tessa Timmers[1,2], Hayel Tuncel[1], Chris WJ van der Weijden[3], Patrick Schober[4], Robert C Schuit[1], Wiesje M van der Flier[2,5], Albert D Windhorst[1], Adriaan A Lammertsma[1], Bart NM van Berckel[1] and Ronald Boellaard[1,3]

Abstract

Accumulation of amyloid beta (Aβ) is one of the pathological hallmarks of Alzheimer's disease (AD), which can be visualized using [^{18}F]florbetapir positron emission tomography (PET). The aim of this study was to evaluate various parametric methods and to assess their test-retest (TRT) reliability. Two 90 min dynamic [^{18}F]florbetapir PET scans, including arterial sampling, were acquired ($n = 8$ AD patient, $n = 8$ controls). The following parametric methods were used; (reference:cerebellum); Logan and spectral analysis (SA), receptor parametric mapping (RPM), simplified reference tissue model2 (SRTM2), reference Logan (rLogan) and standardized uptake value ratios ($SUV_{r(50–70)}$). $BP_{ND}+1$, DVR, V_T and SUVr were compared with corresponding estimates (V_T or DVR) from the plasma input reversible two tissue compartmental (2T4k_V_B) model with corresponding TRT values for 90-scan duration. RPM ($r^2 = 0.92$; slope = 0.91), Logan ($r^2 = 0.95$; slope = 0.84) and rLogan ($r^2 = 0.94$; slope = 0.88), and SRTM2 ($r^2 = 0.91$; slope = 0.83), SA ($r^2 = 0.91$; slope = 0.88), SUVr ($r^2 = 0.84$; slope = 1.16) correlated well with their 2T4k_V_B counterparts. RPM (controls: 1%, AD: 3%), rLogan (controls: 1%, AD: 3%) and $SUV_{r(50–70)}$ (controls: 3%, AD: 8%) showed an excellent TRT reliability. In conclusion, most parametric methods showed excellent performance for [^{18}F]florbetapir, but RPM and rLogan seem the methods of choice, combining the highest accuracy and best TRT reliability.

Keywords

Amyloid PET, Alzheimer's disease, test–retest design, [^{18}F]florbetapir, parametric imaging methods, PET quantification

Received 13 February 2020; Accepted 17 February 2020

Introduction

Alzheimer's disease (AD) is neuropathologically characterized by cortical amyloid beta (Aβ) deposition, which starts to accumulate approximately 10–20 years before clinical symptoms.[1,2] Aβ can be visualized using [^{18}F] florbetapir positron emission tomography (PET).[3,4] Accurate quantification of Aβ is important for identifying subtle amyloid accumulation, as well as for monitoring disease progression and evaluating (experimental) anti-amyloid disease-modifying therapies.[5–7]

So far, most studies have used semi-quantitative measures for [^{18}F]florbetapir uptake, such as the standardized uptake value ratio (SUVr). However, SUVr

[1]Department of Radiology & Nuclear Medicine, Amsterdam University Medical center location VUmc, The Netherlands
[2]Neurology & Alzheimer Center, Amsterdam Neuroscience, Amsterdam University Medical center location VUmc, The Netherlands
[3]Department of Nuclear Medicine & Molecular Imaging, University Medical Center Groningen, Groningen, The Netherlands
[4]Department of Anaesthesiology, Amsterdam University Medical center location VUmc, Amsterdam, The Netherlands
[5]Epidemiology & Biostatistics, Amsterdam Neuroscience, Amsterdam University Medical center location VUmc, Amsterdam, The Netherlands

*These authors contributed equally to this work.

Corresponding author:
Sander CJ Verfaillie, Department of Radiology & Nuclear Medicine, Amsterdam University Medical center location VUmc, P.O. Box 7057, Amsterdam 1007 MB Amsterdam, The Netherlands.
Email: s.verfaillie@amsterdamumc.nl

may be biased and sensitive to changes in perfusion, which are common in AD, and therefore making it less suitable for longitudinal measurements, where full quantification may be required.[8,9] Recently, it was demonstrated that in vivo kinetics of [^{18}F]florbetapir can best be described by a reversible two tissue compartmental model with fitted blood volume (2T4k_V_B).[8] In addition, it has been shown that the simplified reference tissue model-(SRTM) derived binding potential (BP_{ND}) provides an accurate measure of [^{18}F]florbetapir specific binding, showing less bias and lower test–retest variability than SUVr.[8]

So far, it has not been investigated which parametric imaging method is most optimal for the quantification of [^{18}F]florbetapir. Advantages of parametric images are that these can be used in voxel-by-voxel analyses and to take advantage of the scanner resolution. By contrast, full kinetic modelling and SRTM are non-linear regression-based, and therefore more computationally demanding and more susceptible for noise. [^{18}F]florbetapir is a widely used amyloid-beta radiotracer, and validated parametric imaging methods are important for accurate and robust amyloid-beta quantification, allowing whole brain voxel-based analyses which are important in assessing the efficacy of disease modifying drugs over time. In addition, visual assessment of [^{18}F]florbetapir images using BP_{ND}/R_1 images might be more reliable compared to SUVr images.[10,11] Therefore, the aim of this study was to evaluate the performance of various parametric methods for voxel-by-voxel quantification of [^{18}F]florbetapir kinetics and to assess their test–retest (TRT) repeatability.

Material and methods

Participants

Participants have already been described in a previous study, and existing data were used for the present study.[8] In brief, eight patients with mild to moderate probable AD (MMSE $\geq$ 19) from the Amsterdam Dementia Cohort were included. Screening included vital signs, physical and neurological examinations, medical history, neuropsychological assessment, laboratory measurements, and brain MRI. In addition, eight healthy controls were recruited through advertisements in newspapers. These controls were in good physical health, experienced no cognitive complaints, and met Research Diagnostic Criteria (RDC) for "never mentally ill." Controls underwent a comparable screening as AD patients and were only eligible if results of all clinical tests, including brain MRI and neuropsychological assessment, showed no abnormalities. The study was approved by the Medical Ethics Review Committee of the VU University Medical Center and all subjects provided written informed consent, in line with the Helsinki Declaration of 1975 (and 1983 revised) guidelines.

[^{18}F]florbetapir synthesis

[^{18}F]florbetapir (also named Amyvid or [^{18}F]AV45) was synthesized locally in accordance with Avid Radiopharmaceuticals Investigational quality control release criteria.

Data acquisition

Data were acquired using an Ingenuity TF PET/CT scanner (Philips Medical Systems, Best, The Netherlands). Prior to scanning, two cannulas were inserted, one for intravenous [^{18}F]florbetapir administration, the other for arterial sampling. Each subject underwent two [^{18}F]florbetapir PET scans (interval [mean±SD]: 4 ± 2 weeks). Following a low-dose CT for attenuation correction, a 90-min PET emission scan was acquired after a bolus injection of approximately (mean±SD) 294 ± 27 MBq [^{18}F]florbetapir. Arterial blood was sampled continuously at a rate of 5 mL·min^{-1} for the first 5 min and 2.5 mL·min^{-1} thereafter, using an online detection system. Continuous withdrawal was interrupted briefly (approximately 10 s) for the collection of seven (at 5, 10, 20, 40, 60, 75 and 90 min post injection) manual blood samples of approximately 8 mL, which were used to estimate plasma-to-whole blood ratios and to measure plasma metabolite fractions. A detailed description of the radiometabolite analyses has been given elsewhere.[8] Satisfactory blood data were available for six controls and eight AD patients; detailed information about missing blood data can be found elsewhere.[8] Dynamic PET acquisition was performed in list mode, and images were reconstructed in 22 frames (1×15, 3×5, 3×10, 4×60, 2×150, 2×300, 7×600 s) with a matrix size of $128 \times 128 \times 90$ voxels, and were subsequently reconstructed using 3D RAMLA (voxel size of $2 \times 2 \times 2$mm^3). During reconstruction, all usual corrections, e.g. for attenuation, scatter, randoms, decay and dead time were performed. For brain tissue segmentation, 3D T1-weighted structural MRI scans (MPRAGE sequence) were acquired using a 3.0 Tesla Signa HDxt MRI (General Electric, Milwaukee, WI, USA).

Image analysis

Structural 3D T1-weighted MRI images were co-registered and superimposed to the PET images. Subsequently, PVElab was used to derive time activity curves (TACs) in anatomically based regions of interest (Hammers brain atlas, $n = 68$ ROIs).[12] Based on earlier

findings, and as reference, the 2T4k_V_B model was used to obtain plasma-input-derived distribution volume ratio (DVR), and SRTM was used to derive BP_{ND} (using cerebellum grey matter as reference region). In addition, the following plasma input parametric imaging methods were evaluated: Logan, spectral analyses (SA) (both 90 and 60 min), together with the following reference input parametric imaging methods: receptor parametric mapping (RPM), SRTM2, reference Logan (rLogan), multilinear reference tissue model (MRTM) 0, MRTM1, MRTM2, MRTM3A, MRTM3B (all 90 min) and $SUVr_{50\text{-}70}$.[13–18] For MRTM implementations, a scan duration of 90 min was used in order to have sufficient data points for fitting the model. For Logan, rLogan, RPM, SRTM2, and spectral analyses, fitting parameters (such as starting times for linear fits and number of basis functions) were optimized with reference to 2T4k_V_B and SRTM. Cerebellar grey matter was used as reference region. The following bilateral anatomical regions from the Hammers atlas were excluded from analyses because these either did not consist of (cortical) grey matter tissue or/and are devoid of amyloid pathology under normal conditions: caudate nucleus, nucleus accumbens, putamen, thalamus, pallidum, corpus callosum, ventricles and brainstem.[19,20] Finally 52 ROIs remained for image analyses. In addition, [^{18}F]florbetapir $SUV_{50–70}$ images were read for Aβ pathology by an experienced nuclear medicine physician (BvB) to determine the level of amyloid burden in each participant for descriptive purposes.

Statistical analyses

Statistical analyses were performed using SPSS version 20.0.0 (IBM Corp., Armonk New York, USA). χ^2-tests were used for discrete variables, and *t*-tests for continuous demographic and clinical data. To evaluate the suitability of frequently used reference regions for [^{18}F]florbetapir,[21] *t*-tests were used to compare 2T4k_V_B V_T values for cerebellum (1. grey matter [GM], 2. white matter [WM], 3. grey + white matter [GMWM], 4. subcortical WM, 5. brainstem and 6. pons between AD and controls). We first investigated the most optimal parametric imaging method, correlations (explained variance, r^2) and slopes (i.e. bias) between 2T4k_V_B DVR values and SRTM BP_{ND} and various parametric imaging methods (RPM, SRTM2, rLogan, Logan, SA, $SUVr_{50\text{-}70}$ and all MRTM methods) for controls, AD patients and across groups. For correlational analyses, scaling differences between DVR and BP_{ND} ($DVR = BP_{ND} + 1$) are adjusted throughout the remainder of the manuscript. To investigate the impact of scan duration, DVR values obtained with RPM, SRTM2, RLogan, Logan and SA using 60 min of data were compared with those of 90 min scan data.

Results

Clinical and demographic data are presented in Table 1. There were no differences in age (controls = 63 ± 4, AD = 67 ± 6) or sex (three males and five females in both groups) between patients with AD and controls (all $p > 0.05$). Visual assessment of the [^{18}F]florbetapir $SUV_{50–70}$ images showed that all AD patients showed abnormal amyloid accumulation, whereas none of the controls showed significant cortical [^{18}F]florbetapir uptake (see example Figure 1).

There were no significant differences between AD and controls with regard to the reference regions 2T4k_V_B-derived V_t values (Figure 2; cerebellum GM $p = 0.96$, cerebellum WM $p = 0.21$; cerebellum GMWM $p = 0.79$; brainstem $p = 0.12$; pons $p = 0.16$; subcortical WM $p = 0.19$). Subsequent analyses were performed using cerebellum GM as a reference region because this region showed the least differences between groups.

Comparisons between parametric values obtained using different parametric methods and 2T4k_V_B

Table 1. Clinical and demographic data and settings of parametric methods.

Clinical and demographic information	Controls ($n = 8$)	AD patients ($n = 8$)	*p*-value
Age	63 (4)	67 (6)	p=0.17
Males/females *n* (% males)	3/5 (38%)	3/5 (38%)	n.a.
MMSE score	30 (1)	23 (3)	p<0.001
Amyloid burden (% yes)	0/8 (0%)	8/8 (100%)	n.a.
Settings parametric methods			
RPM/SRTM2	0.01–0.1, 50 basis functions		
rLogan/Logan	30–90 min		
Spectral analyses (SA)	0.000167–0.008 (start-end), 50 basis functions		

Note: Data are presented as mean (SD) or as frequency (percentages).

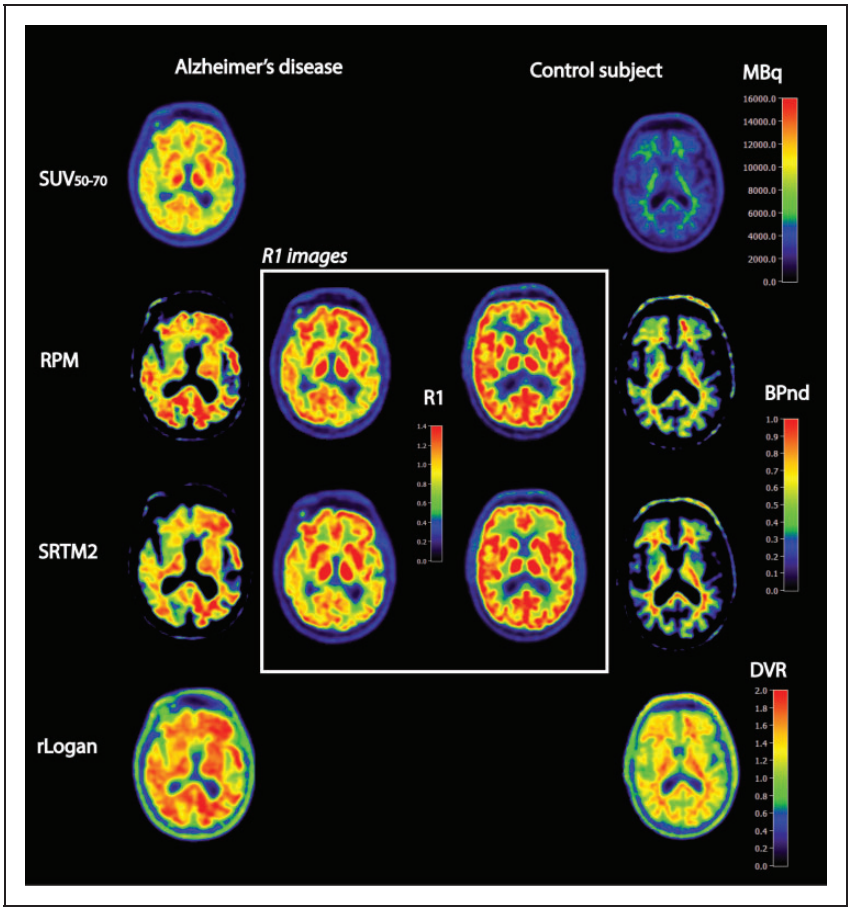

Figure 1. Examples of several quantitative images of a selection of parametric methods for a typical Alzheimer's disease subject and a healthy volunteer. If available (RPM, SRTM2), we also presented (in the center white box) the corresponding R1 images reflecting tracer delivery or relative cerebral blood flow.

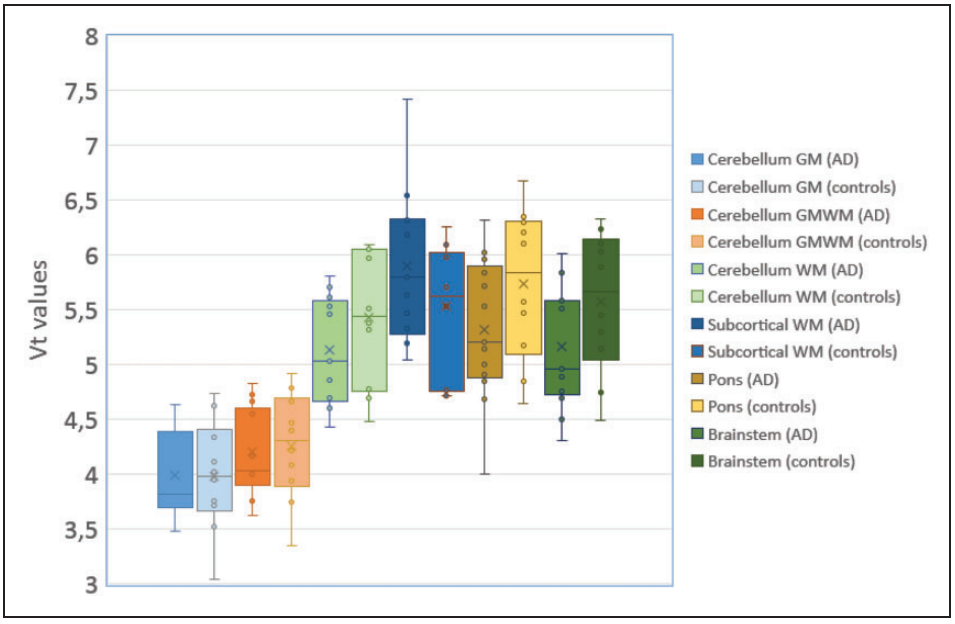

Figure 2. Boxplot and whisker plots with interquartile ranges for V_T values for various reference regions in AD and controls. V_T values were based on 2T4k_V_B model estimations using an original input function.

Table 2. Correlations and test–retest results between 2T4k_V_B-derived DVR values and those seen with the tested parametric methods.

Parametric methods	All subjects r^2 (slope)	Controls r^2 (slope)	TRT (%)	AD r^2 (slope)	TRT (%)
$SUVr_{50–70}$	0.92	0.84	3.35	0.85	7.78
	1.16	1.06		1.12	
90 min					
RPM	0.95	0.84	1.09	0.92	3.05
	0.92	0.88		0.91	
SRTM2	0.91	0.61	1.12	0.88	2.07
	0.83	0.61		0.83	
rLogan	0.94	0.77	0.85	0.90	3.33
	0.88	0.75		0.85	
SA	0.91	0.70	8.12	0.92	18.19
	0.88	0.83		0.92	
Logan	0.95	0.86	9.43	0.93	16.25
	0.84	0.79		0.80	
MRTM0	0.92	0.76	0.88	0.86	3.17
	1.03	1.01		1.00	
MRTM1	0.93	0.83	0.62	0.87	3.8
	0.97	0.95		0.93	
MRTM2	0.83	0.47	2.04	0.74	3.29
	0.96	0.76		0.89	
MRTM3A	0.91	0.74	0.58	0.91	2.88
	1.01	0.93		1.00	
MRTM3B	0.85	0.53	1.62	0.77	2.69
	0.98	0.84		0.94	
60 min					
RPM	0.90	0.73	0.69	0.84	2.58
	0.92	0.86		0.92	
SRTM2	0.88	0.51	1.10	0.83	1.88
	0.81	0.54		0.79	
rLogan	0.90	0.64	0.77	0.84	2.15
	0.84	0.66		0.81	
SA	0.79	0.70	7.73	0.65	17.46
	0.85	0.72		0.80	
Logan	0.88	0.75	8.22	0.82	14.57
	0.78	0.65		0.71	

Note: Parametric methods in comparison to plasma input-derived 2T4k_V_B (V_T or DVR values) using 90 min scan data. The following optimized settings were used for each parametric method (RPM= 0.01–0.1, 50 basis functions; SRTM2 = 0.01–0.1, 50 basis functions; rLogan = 30–90 min; Logan = 30–90 min; Spectral analyses = 0.000167–0.008 (start-end), 50 basis functions. Test–retest results were based upon the average variation of all regions of interest.

(including slopes and intercepts) are presented in Table 2. Across groups, RPM DVR values showed the highest correlations and least bias ($r^2 = 0.95$ and slope = 0.92) compared with 2T4k_V_B-derived DVR values (Figure 3). In addition, Logan ($r^2 = 0.95$; slope = 0.84), rLogan ($r^2 = 0.94$; slope = 0.88), SRTM2 ($r^2 = 0.91$; slope = 0.83), $SUVr_{50–70}$ ($r^2 = 0.92$; slope = 0.79) and SA ($r^2 = 0.91$; slope = 0.88) correlated well with 2T4k_V_B values. The results remained essentially unchanged when reducing the scanning time from 90 to 60 min (Table 2 and 3; Figure 3) or when performing separately for each diagnostic group, and with adequate tracer delivery (i.e. R_1 images) based on RPM and SRTM2 (Figure 1). MRTM models, particularly MRTM1, correlated well with 2T4k_V_B values, but generated noisy (visually) parametric images (data not shown). In a different set of analyses, parametric methods were compared with SRTM BP_{ND} (Table 3). Across groups, based on both 60- and 90-min data, RPM (Figure 3(b) and (d)) and rLogan provided the most accurate results.

Finally, we compared DVR TRT for various parametric methods (Figure 4; Table 2). RPM, SRTM2 and rLogan provided excellent TRT performance for both

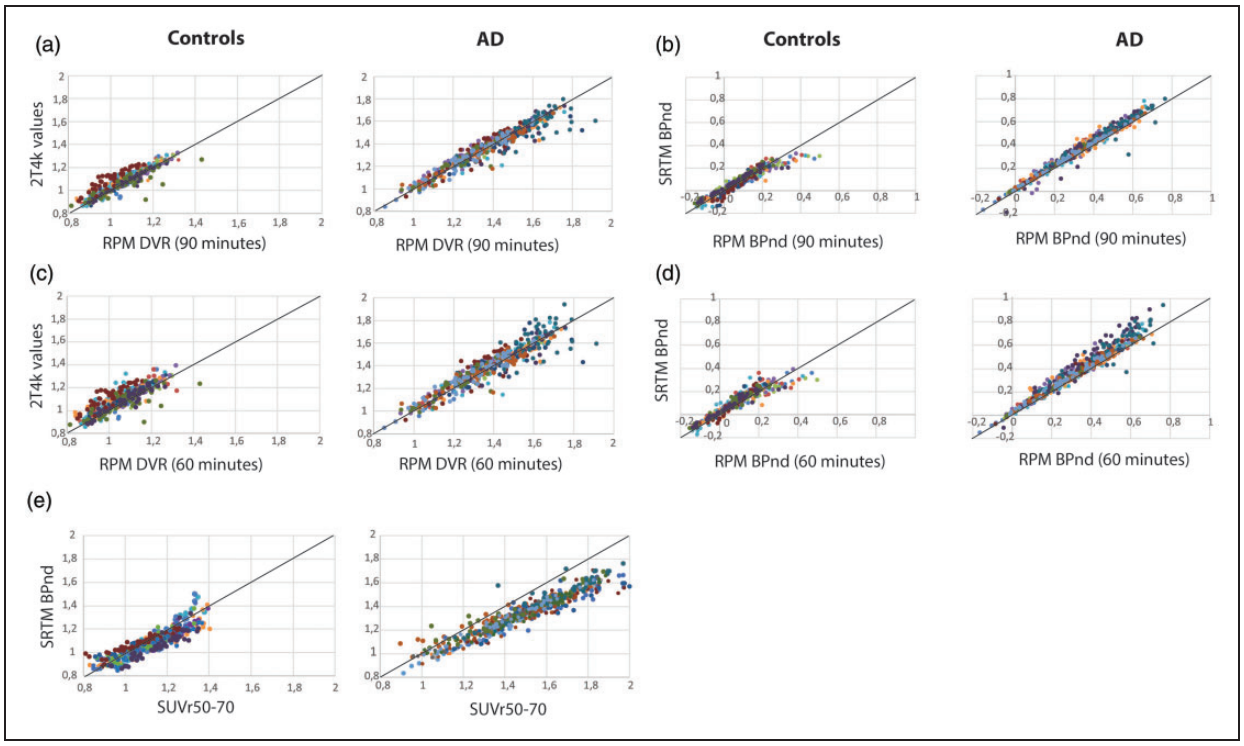

Figure 3. Correlations between RPM DVR (panel A and C [controls and AD patients respectively]), 2T4k_V_B-derived DVR and, RPM BP_{ND} (panel B and D) and SRTM BP_{ND} for +1both 90- and 60-min scan durations and for both AD patients and controls. Panel E shows correlations between SRTM BP_{ND} and $SUVr_{50–70}$. Different colours reflect different regional estimations of each participant.

Table 3. Correlations between SRTM-derived BP_{ND} and those seen with the tested parametric methods.

Parametric methods	All subjects r^2 (slope)	Controls r^2 (slope)	AD r^2 (slope)
$SUVr_{50–70}$	0.93	0.79	0.91
	1.30	0.99	1.25
90 min			
RPM	0.98	0.91	0.98
	1.03	0.88	1.03
SRTM2	0.94	0.78	0.95
	0.94	0.65	0.92
rLogan	0.97	0.89	0.97
	0.99	0.77	0.96
SA	0.64	0.19	0.59
	4.15	2.39	4.45
Logan	0.74	0.35	0.66
	4.15	2.85	4.08
MRTM0	0.96	0.88	0.95
	0.95	1.14	0.97
MRTM1	0.95	0.85	0.95
	0.89	1.00	0.89
MRTM2	0.92	0.72	0.93
	0.90	0.87	0.90
MRTM3A	0.96	0.86	0.97
	0.95	1.01	0.96
MRTM3B	0.32	0.08	0.91
	0.38	0.08	0.95
60 min			
RPM	0.96	0.89	0.95
	1.05	0.90	1.06
SRTM2	0.92	0.70	0.91
	0.91	0.59	0.89
rLogan	0.95	0.84	0.94
	0.96	0.72	0.93
SA	0.67	0.35	0.54
	4.45	2.88	4.39
Logan	0.77	0.40	0.68
	4.10	2.72	3.95

Note: Parametric methods compared to SRTM using 90 min scan data. The following optimized settings were used for each parametric method (RPM= 0.01–0.1, 50 basis functions; SRTM2 = 0.01–0.1, 50 basis functions; rLogan = 30–90 min; Logan = 30–90 min; Spectral analyses = 0.000167–0.008 (start-end), 50 basis functions.

60- and 90-min data (TRT < 5%), and MRTM models for 90-min data. Larger TRT variability was found for plasma input-based methods, i.e. Logan and spectral analyses (TRT range; 7–18%).

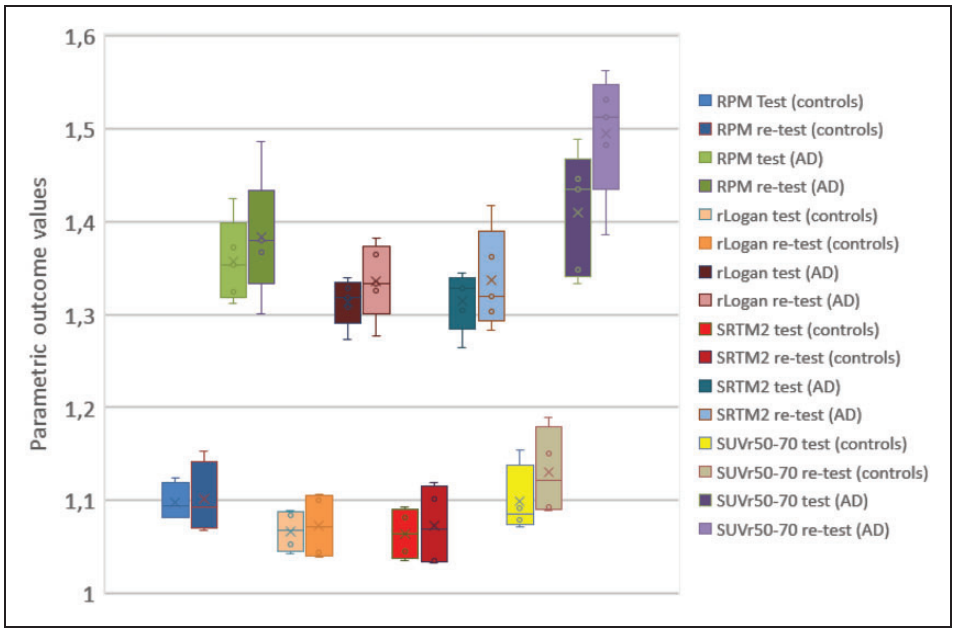

Figure 4. Boxplot and whisker plots with interquartile ranges for test and retest scans (all grey matter voxels) for AD and controls. For RPM and SRTM2 outcome values were rescaled (DVR= BPnd + 1) for illustration purposes. For rLogan DVR values are shown.

Discussion

In this study, we investigated the performance and TRT of various parametric methods for quantifying [^{18}F]florbetapir uptake in both mild to moderate AD patients and controls. In general, amongst reference tissue parametric methods, most parametric methods showed excellent performance, but RPM and rLogan showed the least bias compared with corresponding 2T4k_V_B and SRTM estimates, together with excellent TRT performance. Plasma input parametric methods showed slightly more bias and lower TRT repeatability, with best results obtained for Logan.

We used a number of approaches to evaluate various parametric methods. Firstly, we validated each (plasma input) parametric method against the reversible two tissue compartmental model-(2T4k_V_B) derived DVR and SRTM-derived BP_{ND}. In order to assess various levels of [^{18}F]florbetapir binding, we performed comparisons across groups as well as for AD and controls separately. Across groups, all parametric methods (particularly RPM, MRTM0, MRTM1 and MRTM3A with r^2>0.90 and slopes ~1.00) corresponded well with relatively low bias relative to 2T4k_V_B-derived DVR and SRTM-derived BP_{ND}. Parametric methods based on linearization techniques (i.e. rLogan, Logan) (slightly) underestimated [^{18}F]florbetapir binding compared with both 2T4k_V_B-derived DVR and SRTM-derived BP_{ND}, which is in line with another study using linearization techniques.[22] Of these linearization techniques, rLogan provided the highest accuracy (lowest bias) compared with both 2t4k and SRTM (non-linear). RPM showed the best performance of the basis function approaches (i.e. RPM, SRTM2, SA). In contrast to previous studies, methods fixing the reference k_2' parameter (i.e. MRTM2, SRTM2) did not result in better accuracy and higher precision due to lower levels of noise compared with methods in which k_2' was not fixed (e.g. RPM).[22,23] For our reference tissue methods, we used cerebellum grey matter, because pathological studies have demonstrated that the cerebellum is usually devoid of amyloid pathology in mild to moderate AD.[24–26] In agreement with literature, we did not find any significant differences between cerebellar Vt values between AD and controls, which suggests that this region can be used as a valid reference region. In general, accuracy seemed highest in the AD group for most parametric methods, which can be explained by the higher DVR values due to substantial amyloid accumulation in AD patients that are less susceptible to small changes. The present findings are in line with earlier studies on other amyloid tracers ([^{11}C]PiB and [^{18}F]flutemetamol), particularly with respect to the performance of rLogan and RPM.[27–29] Although we observed slightly lower correlations and positive bias between SUVr and corresponding 2T4k_V_B and SRTM-based DVR values, there was still a good agreement. One explanation is that SUVr is susceptible to (altered) brain perfusion,[6,30] which is commonly present in AD.[31] This could affect tracer delivery and

kinetics, and could result in bias compared with quantitative methods.

Next, we evaluated TRT performance for [^{18}F]florbetapir, showing larger TRT variability in AD than in controls. This is probably due to the negligible [^{18}F]florbetapir binding in controls, which has also been confirmed by visual readings.[32] TRT variability was comparable for DVR and $BP_{ND,}$ but semi-quantitative techniques (SUVr) as well as methods relying on plasma input function (Logan and spectral analyses) showed poorer TRT performance both for AD and controls. These findings are well in line with TRT studies on [^{11}C]PiB, which indicated more variability over time while using semi-quantitative techniques or plasma input models for [^{18}F]florbetapir,[6,27] and could be explained by AD-related hypoperfusion for SUVr or relatively noisy estimations when using plasma input-based models.[8,31]

Finally, we investigated the effects of reducing scanning time from 90 to 60 min. In a previous study, it was shown that reliable SRTM BP_{ND} required a minimum of 60 min of data.[8] Consequently, in the present study, no shorter scanning times were investigated. All quantitative parametric methods, except for spectral analyses, Logan and MRTM models, only showed minor changes in BP_{ND} or DVR for the shorter scan time, which implies that 60 min is sufficient to obtain reliable and valid [^{18}F]florbetapir binding images. In particular, RPM provided comparable results for 60 and 90 min data with excellent TRT performance. Taken together, a dynamic acquisition of 60 min seems sufficient for RPM-derived R_1 and BP_{ND} images, although an extension to 70 min can be considered to allow for the generation of $SUVr_{50–70}$ images (FDA recommended interval for static [^{18}F]florbetapir scans).

In summary, various parametric methods showed excellent performance for [^{18}F]florbetapir, but RPM and rLogan are methods of choice for generating parametric images with excellent TRT performance particularly in AD patients and for reduced scan duration. These findings illustrate reliable ways to accurately quantify amyloid deposition, and are especially relevant for capturing regional changes of amyloid over time, for example for disease modifying therapies and clinical trials.

Funding

The author(s) disclosed receipt of the following financial support for the research, authorship, and/or publication of this article: Van der Flier received grant support from ZonMW, NWO, EU-FP7, Alzheimer Nederland, CardioVascular Onderzoek Nederland, Stichting Dioraphte, Gieskes-Strijbis Fonds, Boehringer Ingelheim, Piramal Neuroimaging, Roche BV, Janssen Stellar and Combinostics. All funding is paid to the institution.

Acknowledgements

This research was made possible by Avid Radiopharmeuticals Inc., a wholly owned subsidiary of Eli Lilly and Company (NYSE: LLY). Research of the VUmc Alzheimer Center is part of the neurodegeneration research program of the Amsterdam Neuroscience. We would like to acknowledge the participants of the Amsterdam Dementia Cohort and the healthy volunteers for dedicating their time and energy to this study.

Declaration of conflicting interests

The author(s) declared no potential conflicts of interest with respect to the research, authorship, and/or publication of this article.

Authors' contributions

Sander CJ Verfaillie: acquiring data, analysing and interpreting data, drafting the manuscript, approving the final content of the manuscript. Sandeep SV Golla: acquiring data, analysing and interpreting data, drafting the manuscript, approving the final content of the manuscript. Chris Van der Weijden: acquiring data, analysing and interpreting data, critically revising the manuscript, approving the final content of the manuscript. Tessa Timmers: acquiring data, analysing and interpreting data, critically revising the manuscript, approving the final content of the manuscript. Hayel Tuncel: acquiring data, analysing and interpreting data, critically revising the manuscript, approving the final content of the manuscript. Robert C Schuit: acquiring data, analysing and interpreting data, critically contributing to the manuscript, approving the final content of the manuscript. Patrick Schober: acquiring data, critically revising the manuscript, approving the final content of the manuscript. Wiesje M van der Flier: contributing to conception and design, enhancing its intellectual content, approving the final content of the manuscript. Albert D Windhorst: contributing to conception and design, enhancing its intellectual content, approving the final content of the manuscript. Adriaan A Lammertsma: contributing to conception and design, analysing and interpreting data, drafting the manuscript and enhancing its intellectual content, approving the final content of the manuscript. Bart NM van Berckel: contributing to conception and design, analysing and interpreting data, drafting the manuscript and enhancing its intellectual content, approving the final content of the manuscript. Ronald Boellaard: contributing to conception and design, analysing and interpreting data, drafting the manuscript and enhancing its intellectual content, approving the final content of the manuscript. Boellaard is the principal investigator of this study.

The author(s) declared the following potential conflicts of interest with respect to the research, authorship, and/or publication of this article: Verfaillie, Golla, Timmers, Tuncel, Schuit, Schober, Windhorst, Lammerstma, Boellaard and van Berckel report no conflict of interest.

ORCID iDs

Sander CJ Verfaillie https://orcid.org/0000-0003-1820-3378
Adriaan A Lammertsma https://orcid.org/0000-0003-1237-2891

References

1. Jack CR, Knopman DS, Jagust WJ, et al. Tracking pathophysiological processes in Alzheimer's disease: an updated hypothetical model of dynamic biomarkers. *Lancet Neurol* 2013; 12: 207–216.
2. Bateman RJ, Xiong C, Benzinger TLS, et al. Clinical and biomarker changes in dominantly inherited Alzheimer's disease. *N Engl J Med* 2012; 367: 795–804.
3. Wong DF, Rosenberg PB, Zhou Y, et al. In vivo imaging of amyloid deposition in Alzheimer disease using the radioligand 18F-AV-45 (Flobetapir F 18). *J Nucl Med* 2010; 51: 913–920.
4. Yang L, Rieves D and Ganley C. Brain amyloid imaging – FDA approval of florbetapir F18 injection. *N Engl J Med* 2012; 367: 885–887.
5. Lammertsma AA. Forward to the past: the case for quantitative PET imaging. *J Nucl Med* 2017; 58: 1019–1024.
6. van Berckel BNM, Ossenkoppele R, Tolboom N, et al. Longitudinal amyloid imaging using 11C-PiB: methodologic considerations. *J Nucl Med* 2013; 54: 1570–1576.
7. Mattsson N, Insel PS, Landau S, et al. Diagnostic accuracy of CSF Ab42 and florbetapir PET for Alzheimer's disease. *Ann Clin Transl Neurol* 2014; 1: 534–543.
8. Golla SSV, Verfaillie SCJ, Boellaard R, et al. Quantification of [18F]florbetapir: a test-retest tracer kinetic modelling study. *J Cereb Blood Flow Metab* 2019; 39: 2172–2180.
9. Ottoy J, Verhaeghe J, Niemantsverdriet E, et al. Validation of the semiquantitative static SUVR method for ^{18}F-AV45 PET by pharmacokinetic modeling with an arterial input function. *J Nucl Med* 2017; 58: 1483–1489.
10. Collij L, Konijnenberg E, Reimand J, et al. Assessing amyloid pathology in cognitively normal subjects using [^{18}F]flutemetamol PET: comparing visual reads and quantitative methods. *J Nucl Med* 2019; 60: 541–547.
11. Zwan MD, Ossenkoppele R, Tolboom N, et al. Comparison of simplified parametric methods for visual interpretation of 11C-Pittsburgh compound-B PET images. *J Nucl Med* 2014; 55: 1305–1307.
12. Hammers A, Allom R, Koepp MJ, et al. Three-dimensional maximum probability atlas of the human brain, with particular reference to the temporal lobe. *Hum Brain Mapp* 2003; 19: 224–247.
13. Innis RB, Cunningham VJ, Delforge J, et al. Consensus nomenclature for in vivo imaging of reversibly binding radioligands. *J Cereb Blood Flow Metab* 2007; 27: 1533–1539.
14. Gunn RN, Lammertsma AA, Hume SP, et al. Parametric imaging of ligand-receptor binding in PET using a simplified reference region model. *Neuroimage* 1997; 6: 279–287.
15. Lammertsma AA and Hume SP. Simplified reference tissue model for PET receptor studies. *Neuroimage* 1996; 4: 153–158.
16. Logan J, Fowler JS, Volkow ND, et al. Distribution volume ratios without blood sampling from graphical analysis of PET data. *J Cereb Blood Flow Metab* 1996; 16: 834–840.
17. Ichise M, Liow JS, Lu JQ, et al. Linearized reference tissue parametric imaging methods: application to [11C] DASB positron emission tomography studies of the serotonin transporter in human brain. *J Cereb Blood Flow Metab* 2003; 23: 1096–1112.
18. Cunningham VJ and Jones T. Spectral analysis of dynamic PET studies. *J Cereb Blood Flow Metab* 1993; 13: 15–23.
19. Dugger BN, Clark CM, Serrano G, et al. Neuropathologic heterogeneity does not impair florbetapir-positron emission tomography postmortem correlates. *J Neuropathol Exp Neurol* 2014; 73: 72–80.
20. Braak H and Braak E. Neuropathological stageing of Alzheimer-related changes. *Acta Neuropathol* 1991; 82: 239–259.
21. Landau SM, Fero A, Baker SL, et al. Measurement of longitudinal-amyloid change with 18F-Florbetapir PET and standardized uptake value ratios. *J Nucl Med* 2015; 56: 567–574.
22. Slifstein M and Laruelle M. Effects of statistical noise on graphic analysis of PET neuroreceptor studies. *J Nucl Med* 2000; 4: 2083–2088.
23. Ichise M, Toyama H, Innis RB, et al. Strategies to improve neuroreceptor parameter estimation by linear regression analysis. *J Cereb Blood Flow Metab* 2002; 22: 1271–1281.
24. Wegiel J, Wisniewski HM, Dziewiatkowski J, et al. Cerebellar atrophy in Alzheimer's disease – clinicopathological correlations. *Brain Res* 1999; 818: 41–50.
25. Murray ME, Lowe VJ, Graff-Radford NR, et al. Clinicopathologic and 11C-Pittsburgh compound B implications of Thal amyloid phase across the Alzheimer's disease spectrum. *Brain* 2015; 138(Pt 5): 1370–1381.
26. Thal DR, Rüb U, Orantes M, et al. Phases of Aβ-deposition in the human brain and its relevance for the development of AD. *Neurology* 2002; 58: 1791–1800.
27. Tolboom N, Yaqub M, Boellaard R, et al. Test-retest variability of quantitative [11C]PIB studies in Alzheimer's disease. *Eur J Nucl Med Mol Imaging* 2009; 36: 1629–1638.

28. Price JC, Klunk WE, Lopresti BJ, et al. Kinetic modeling of amyloid binding in humans using PET imaging and Pittsburgh Compound-B. *J Cereb Blood Flow Metab* 2005; 25: 1528–1547.
29. Heurling K, Buckley C, Van Laere K, et al. Parametric imaging and quantitative analysis of the PET amyloid ligand [18F]flutemetamol. *Neuroimage* 2015; 121: 184–192.
30. Carson RE, Channing MA, Blasberg RG, et al. Comparison of bolus and infusion methods for receptor quantitation: application to [18F]cyclofoxy and positron emission tomography. *J Cereb Blood Flow Metab* 1993; 13: 21–42.
31. Verfaillie SCJ, Adriaanse SM, Binnewijzend MAA, et al. Cerebral perfusion and glucose metabolism in Alzheimer's disease and frontotemporal dementia: two sides of the same coin? *Eur Radiol* 2015; 25: 3050–3059.
32. Ossenkoppele R, Jansen WJ, Rabinovici GD, et al. Prevalence of amyloid PET positivity in dementia syndromes: a meta-analysis. *JAMA* 2015; 313: 1939–1949.